Pergamon

0956-7151(94)00385-8

Acta metall. mater. Vol. 43, No. 5, pp. 1817–1823, 1995

0956-7151/95 $9.50 + 0.00

THE INFLUENCE OF AN ORDERING TRANSITION ON THE INTERDIFFUSION IN Au–Cu ALLOYS

B. STRAUMAL, E. RABKIN, W. GUST and B. PREDEL

Max-Planck-Institut für Metallforschung and Institut für Metallkunde, Seestr. 75, D-70174 Stuttgart, Germany

(Received 18 November 1993; in revised form 16 September 1994)

Abstract—The concentration dependencies of the interdiffusion coefficient, $\tilde{D}(c)$, have been determined with the aid of electron probe microanalysis at 11 temperatures above and below the temperature T_{ord} of the A1–L1$_2$ (Cu_3Au) ordering transition. At temperatures $T > T_{ord}$ there are minima on these dependencies near the Cu_3Au composition. Slightly below T_{ord} the $\tilde{D}(c)$ dependencies are monotonous. At $T < (T_{ord} - 20\,K)$ maxima appear on $\tilde{D}(c)$ which grow with decreasing temperature. Such a behaviour is explained by the concentration dependence of the thermodynamic factor Φ. Dependencies $\Phi(c, T)$ have been calculated within the framework of the tetrahedron approximation of the cluster variation method. The calculated dependencies are in good agreement with the experimental data.

1. INTRODUCTION

Due to the increased resistance to plastic deformation at elevated temperatures and other properties which originate from the strong bonding between the dissimilar constituent atoms many ordered intermetallic compounds are attractive materials for a wide range of engineering applications [1–3]. The application of these materials in advanced aerospace structures and propulsion systems are only possible because they show reduced atomic mobilities at elevated temperatures [4, 5]. Unfortunately, the laws governing the diffusional properties of ordered intermetallic compounds are still poorly understood. For example, the self-diffusion coefficients in these materials have only a slight minimum on the stoichiometric concentration (CoAl [6], Ni_3Al [7]), but the interdiffusion coefficients $\tilde{D}$ which actually define the high-temperature properties of such important intermetallics like NiAl, CoAl and FeAl depend strongly on the deviations from stoichiometry: $\tilde{D}$ can increase or decrease by more than a factor of ten in the *narrow concentration interval* where the intermetallic compound exists [8, 9]. These dependencies of $\tilde{D}$ on the concentration c are also very unusual; for example, $\tilde{D}(c)$ has a deep minimum near the stoichiometric concentration in NiAl [8], but in Ni_3Nb $\tilde{D}(c)$ has a strong maximum at 75 at.%Ni [9]. Also well known is the drastic influence of small ternary additions on the properties of ordered compounds [5].

Another important open question is the unusual behaviour of the coefficients of bulk and grain boundary diffusion in the *narrow temperature interval* near the temperature of ordering phase transition, T_{ord}, particularly because the coefficients of self-diffusion normally do not have any anomalies [10–12].

The goal of this work was to investigate the behaviour of the interdiffusion coefficient in the *narrow temperature interval* near the bulk ordering transition and in the *narrow concentration interval* where the ordered phase exists. For this sake, we have measured the concentration dependencies $\tilde{D}(c)$ above and below T_{ord} and have developed a method for description and prediction of $\tilde{D}(c)$ peculiarities using existing thermodynamic data. For the measurements and theoretical calculations we have chosen the A1–L1$_2$ (Cu_3Au) ordering phase transition in the Au–Cu system because the phase diagram, self-diffusion coefficients and thermodynamic data for this classic system are well established. On the other hand, many technologically important ordered compounds like, for example, Ni_3Al, Ni_3Ga and $(Co, Fe)_3V$ also have the same L1$_2$ structure [14].

2. EXPERIMENTAL

This work is devoted to the investigation of bulk interdiffusion near the A1–L1$_2$ ordering phase transition in Au–Cu alloys. Cylindrical single crystals (10 mm diameter) were grown from Cu of 99.9998% purity by the Bridgman technique in high-purity graphite crucibles and oriented by Laue X-ray back-reflection. Samples, approximately 2 × 2.2 × 7 mm in size, had the 2.2 × 7 mm faces parallel to {011} cut from the single crystals. The samples were carefully polished on 4000 grid SiC paper. After cleaning, the samples were annealed for 15 h at 1223 K in order to relieve residual strains.

The Cu–56 at.%Au alloy was produced from Au of 99.998% purity and Cu as mentioned above. This alloy has the lowest solidus temperature (1162 K) in the Cu–Au system [14]. The alloy was homogenized

in vacuum ($<4 \times 10^{-4}$ Pa) at 1183 K for 100 h, rolled to a thickness of about 0.5 mm and cut to slices of 2×5 mm. These thin slices of Cu–56 at.%Au alloy were then fixed between two single crystalline specimens parallel to {011} [Fig. 1(a)] using a stainless steel holder and encapsulated in silica ampoules under vacuum ($<4 \times 10^{-4}$ Pa). The ampoules were put into a furnace with a temperature of 1183 K for 4 min and subsequently quenched in water. During the 4 min heating ampoules were heated up to 1183 K (about 3.5 min) and annealed at 1183 K for about 30 s. This time was sufficient to melt the slice of Cu–56 at.%Au alloy and to produce a contact between the alloy and both Cu single crystals [Fig. 1(b)]. According to the Cu–Au phase diagram some copper was solved in the film of liquid Cu–Au alloy. After quenching, the concentration c_0, of gold in the transition layer was about 45 at.%. The distance between the positions of contact planes before and after heating was about 60 μm.

The diffusion couple Cu/Cu–45 at.%Au was formed after this procedure. Therefore, the stoichiometric concentration of the ordered phase Cu_3Au ($L1_2$) lies somewhere in the middle of the concentration interval where the interdiffusion was studied.

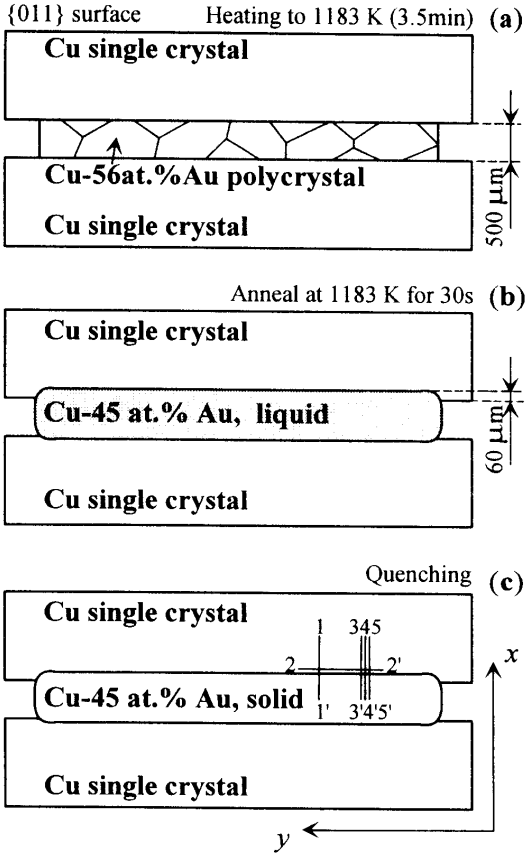

Fig. 1. Sample preparation and determination of the diffusion profiles. (a) Two {011} Cu single crystals fixed together with a slice of Cu–56 at.%Au polycrystal between them. (b) Anneal at 1143 K for 30 s. The intermediate melts, and the surface layer of the Cu single crystals solves into the melt. (c) Solidified Cu–45 at.%Au quasi-single crystal between Cu single crystals after quenching. 1–1′ to 5–5′ are the positions of the line scans used for the determination of the concentration profiles.

It was important to control the thickness of the diffusional layer built between the halves of the diffusion couple during the preparation. The thickness of this layer should be negligible in comparison with the thickness of the diffusional layer after the diffusional anneal because the solution for the couple with two infinite halves and constant concentrations was to be used. During the formation of the diffusion couple ($t = 30$ s) the former contact plane moved 60 μm due to the dissolution of Cu into the Cu–Au alloy. The thickness x_0 of the diffusional layer for diffusion from the plane with constant concentration c_0 moving with velocity v was calculated using the following equation [15]

$$c(x,t) = \frac{1}{2}c_0\left[\operatorname{erfc}\frac{x+vt}{2\sqrt{\tilde{D}t}} + \exp\left(-\frac{vx}{\tilde{D}}\right)\operatorname{erfc}\frac{x-vt}{2\sqrt{\tilde{D}t}}\right]. \quad (1)$$

Here $\tilde{D}(c)$ is the interdiffusion coefficient for the Cu–56 at.%Au alloy extrapolated to 1183 K using experimental data [16]. According to this equation, $x_0 \approx 0.1$ μm. The electron probe microanalysis (EPMA) measurements show that the thickness of the transition layer is indeed negligible in comparison with the thickness of the diffusional layer after the anneal. The EPMA profiles show also that the Au concentration in the quenched layer is constant (see left side of Fig. 2).

Our procedure of sample preparation permits us to investigate the interdiffusion in single crystals without the disturbing influence of GBs in the diffusion zone. Indeed, during the quenching the liquid layer crystallizes on the Cu single crystals like on seeds, and two single crystals of Cu–45 at.%Au grow on both {011} samples. (Of course, these single crystals of Cu–Au alloy are not as perfect as the Cu substrates.)

The diffusion couples were then annealed in the same ampoules at 11 different temperatures above and below the temperature of the A1–$L1_2$ ordering transition ($T_{ord} = 663$ K [14]). After annealing the samples were mounted in Wood's metal and ground and polished with 1 μm diamond paste. The concentration profiles $c(x)$ [Figs 1(c) and 2] in the diffusion layer perpendicular to the contact plane were then determined. The EPMA measurements were carried out by wave length dispersive analysis on a JEOL 6400 electron probe microanalyser operated at 15 kV. The intensities of the Au M_α and Cu L_α peaks were determined. The Au and Cu concentrations were obtained utilizing a program which applied atomic number, absorption, fluorescence and background corrections.

The dependencies of the interdiffusion coefficient $\tilde{D}$ on the molar fraction of Au atoms c were then calculated using the concentration profiles $c(x)$. In order to improve the accuracy of $\tilde{D}(c)$ determination and to avoid effects connected with the deviation of

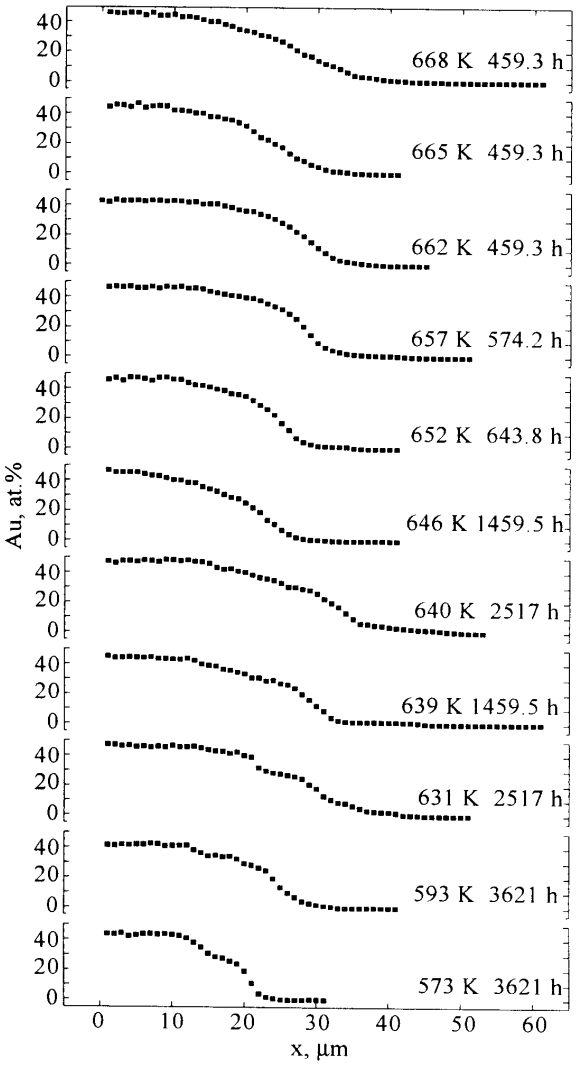

Fig. 2. Dependencies of the Au concentration c in the diffusion zone on the distance x for the temperatures studied.

the shape of the contact interface from the ideal plane, the following measuring procedure was applied [Fig. 1(c)]. Firstly, the concentration profile $c(x)$ perpendicular to the contact plane was measured [profile 1–1′ in Fig. 1(c)] in order to localize the area with the largest local concentration gradient (where c decreases from ~25 to 20 at.%Au). Then the concentration profile $c(y)$ along the contact plane was measured [profile 2–2′ in Fig. 1(c)] in order to localize the location where $c(y) = \text{const}$ on the long distance. After that, the other concentration profiles were measured with high accuracy in the middle of the place with $c(y) = \text{const}$ [profiles 3–3′, 4–4′ and 5–5′ in Fig. 1(c)]. For the determination of the concentration profiles the electron beam was stepped at 1 μm intervals, the distance between the profiles was 2 μm. For each group of neighbouring profiles the averaged profile was then determined.

The averaged profiles were processed in order to determine the concentration dependence of the interdiffusion coefficient $\tilde{D}(c)$. We have employed the Boltzmann–Matano analysis for the calculation of $\tilde{D}(c)$. The method can be applied only if Vegard's rule for the molar volume of alloys is valid. It has been shown recently [9] that even in the case of relatively strong deviations from the Vegard's rule (about 2%) the difference between the Boltzmann–Matano analysis and exact Sauer–Freise [17] analysis is negligible. Thus, in the present work the Boltzmann–Matano method has been used. In order to smooth the experimental data, the concentration tails of the diffusion profiles were fitted by the error function (Hall method [18]), and the rest of the profile was smoothed by a four-point Fourier filter. The interdiffusion coefficient $\tilde{D}$ for the given Au concentration c^* at the given distance x^* was calculated according to the formula.

$$\tilde{D}(c^*) = \left(2t \frac{\partial c}{\partial x}\bigg|_{x^*}\right)^{-1} \int_0^{c^*} (x_M - x)\, dc \qquad (2)$$

where t is the time of the diffusion anneal, x is the distance and x_M denotes the position of the Matano plane which is defined by

$$\int_0^{c_0} (x_M - x)\, dc = 0 \qquad (3)$$

where c_0 is the molar fraction of Au atoms in the Au-rich foil used for the preparation of the diffusional couple.

3. RESULTS

The averaged concentration profiles $c(x)$ (Fig. 2) are shown for all temperatures investigated. The smoothest profiles are those for 657 and 662 K. All other profiles have different deviations from the error function form typical of $\tilde{D}(c) = \text{const}$. The most prominent irregularities are found for 593 and 573 K. The concentration dependencies of the interdiffusion coefficient $\tilde{D}(c)$ determined using the procedure described above are shown in Fig. 3. The following features can be seen in these dependencies in the Au concentration interval of interest (20–30 at.%Au):

- There are definite minima in these dependencies at temperatures above the critical temperature T_{ord} of the order–disorder transition (663 K).
- Below the critical temperature T_{ord} up to 646 K the concentration dependencies are monotonous.
- Below 646 K a maximum appears at approx. 27 at.%Au. The lower the temperature, the more pronounced is the maximum in $\tilde{D}(c)$.

The concentration dependencies of formally determined activation energy $\tilde{Q}(c)$ and pre-exponential factor $\tilde{D}_0(c)$ for interdiffusion are shown in Figs 4 and 5. At low Au concentrations (in the disordered state, $c < 15$ at.%Au) they nearly do not depend on c ($\tilde{Q} = 120 \pm 10$ kJ/mol and $\tilde{D}_0 = 3 \times 10^{-8}$ m^2/s). Above $c \approx 15$ at.%Au the $\tilde{Q}(c)$ and $\tilde{D}_0(c)$ dependencies are nonmonotonous. Both of them have minima at $c \approx 27$ at.%Au ($\tilde{Q} \approx 60$ kJ/mol and $\tilde{D}_0(c) \approx 10$–$12$ m^2/s). We will see below that the

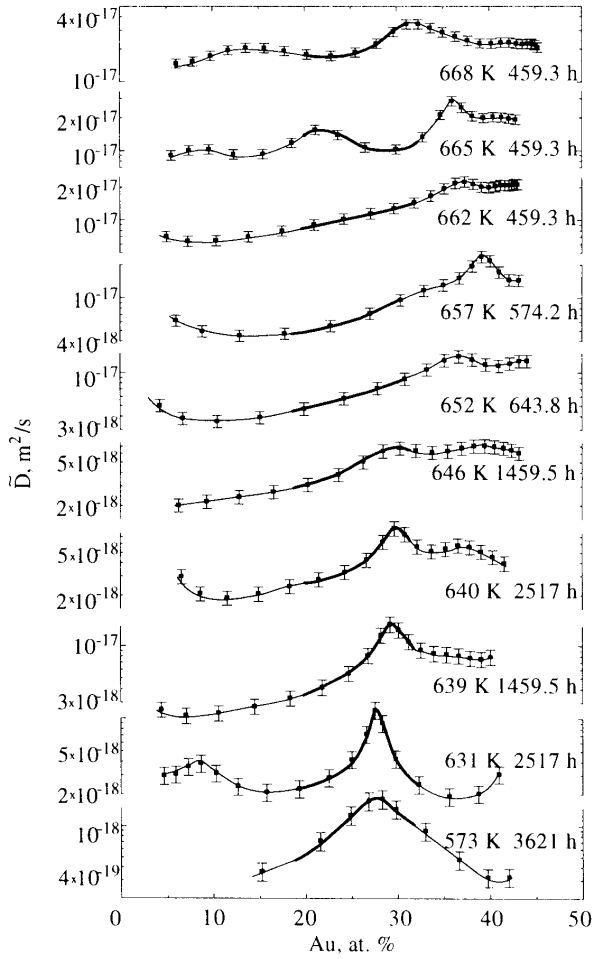

Fig. 3. Dependencies of the interdiffusion coefficient for Cu–Au alloys on the Au concentration. The thick line shows the concentration interval we were interested in.

Arrhenius parameters for interdiffusion have a physical sense only in the interval of concentrations where the alloy is in the disordered state in the whole temperature interval studied.

The temperature dependence of the interdiffusion coefficient $\tilde{D}(T)$ for $c = 10$ at.%Au is shown in

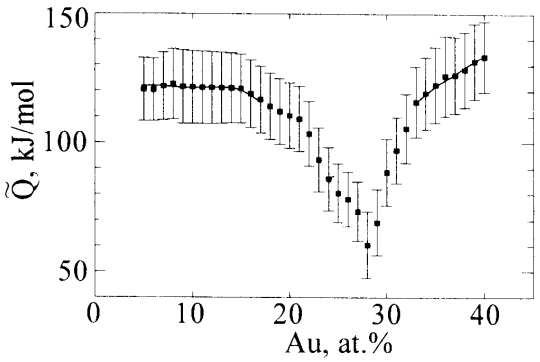

Fig. 4. The activation energy for interdiffusion in Cu–Au alloys as a function of the Au concentration. The low values of the activation energy between 18 and 33 at.%Au are connected with the temperature dependence of the thermodynamic factor Φ and have not any physical background. The error bars are defined by the linear regression procedure.

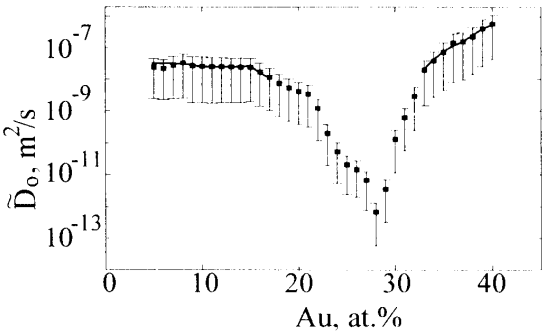

Fig. 5. The pre-exponential factor for interdiffusion in Cu–Au alloys as a function of the Au concentration.

Fig. 6. That composition lies in the disordered region A1 and satisfy the above requirement.

4. DISCUSSION

According to Manning [19] the interdiffusion coefficient can be written as

$$\tilde{D} = (c \cdot D^*_{Cu} + (1 - c) \cdot D^*_{Au})\Phi r \qquad (4)$$

where D^*_{Cu} and D^*_{Au} are tracer self-diffusion coefficients of the components in the homogenous Cu–Au alloy, Φ is the thermodynamic factor and r is the vacancy wind factor which is usually of the order of unity and further will not be taken into account. It is known that tracer self-diffusion coefficients are changing in the ordered state [8]. In the case of magnetic ordering in α-Fe and its alloys the effect was thoroughly investigated [20–22]. Generally, tracer diffusion coefficients in the ordered ferromagnetic state are lower than follows from the extrapolation of the Arrhenius line from the disordered paramagnetic region, and the activation energy for the diffusion far below the transition point is higher than in the disordered state. These features of the self-diffusion coefficient temperature behaviour have also been observed in β-brass [23]. The physical reason for the increase in activation energy is the additional energy necessary for the breaking of atomic bonds in the ordered alloys at the formation and migration of a vacancy. It is generally believed that qualitatively the principal features of the interdiffusion coefficient behaviour at the order–disorder transition are the same as for the self-diffusion coefficient. However,

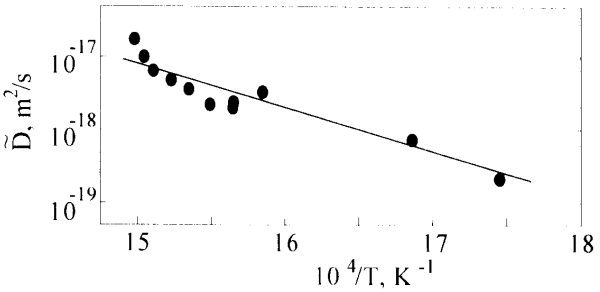

Fig. 6. Arrhenius plot of the interdiffusion coefficient $\tilde{D}$ for Cu–10 at.%Au.

present results show (see Fig. 3) that at some temperatures the interdiffusion coefficient can be higher in the ordered than in the disordered state.

We will demonstrate that the thermodynamic factor Φ is responsible for such a behaviour of the interdiffusion coefficient. Φ expresses the tendency of an alloy to mixing or unmixing and can be written as [15]

$$\Phi = \frac{c(1-c)}{RT}\left(\frac{\partial^2 G}{\partial c^2}\right) \tag{5}$$

where G is the Gibbs energy of the alloy, R is the gas constant and T is the absolute temperature. It can be seen from equation (5) that Φ is proportional to the second derivative of Gibbs energy of an alloy with respect to the concentration. Therefore, it should be connected with the other thermodynamic quantities, like specific heat, which are changing during the phase transformation. It was demonstrated that Φ plays an important role in the vicinity of the critical temperature of unmixing T_{unm}, where the above mentioned second derivative approaches zero. For example, in the Nb–H system the interdiffusion coefficient decreases by several orders of magnitude slightly above T_{unm}, while the self-diffusion coefficient follows the normal Arrhenius dependence [15]. However, till now less attention has been paid to the possible role of the thermodynamic factor at the order–disorder transformation.

4.1. *Calculation of ϕ by the cluster variation method*

For the calculation of the thermodynamic factor, the Gibbs energy of an alloy should be calculated first. For that purpose we have used the tetrahedron approximation of the cluster variation method (CVM) [24]. This is the lowest approximation which allows one to predict the Cu–Au phase diagram correctly. The lower order approximations (pair CVM approximation or Bragg–Williams–Gorsky model) do not take into account the different types of neighbourhood situations in the face centred cubic (f.c.c.) lattice and, therefore, the phase diagrams calculated on their basis are not consistent with the experimental data. We utilized the mean-field formulation of CVM proposed in [24]. The set of spin variables $\{\sigma_i\}$ is introduced such that $\sigma_i = 1$ if the ith site is occupied by a Cu atom and $\sigma_i = -1$ if the ith site is occupied by a Au atom. The contribution of the internal interactions inside the maximal cluster (tetrahedron) and its subclusters (segments and single sites) to the cluster Hamiltonian can be then written as follows

$$H_{\text{clust}} = -v \sum_{i,j \in \text{clust}} \sigma_i \sigma_j \tag{6}$$

where the summation is taken over the nearest neighbours inside the cluster and v is the interaction energy; an irrelevant constant is not taken into account. To the expression in equation (6) the energies corresponding to the interaction of cluster spins with the mean field creating by the other tetrahedra through the common segment i–j

$$-\alpha_k \sigma_i \sigma_j - \beta_k(\sigma_i + \sigma_j) \tag{7}$$

common atom at the site i

$$\gamma_k \sigma_i \tag{8}$$

and with the external field h which plays a role of a chemical potential

$$h\sigma_i \tag{9}$$

should be added. Here $k = 1$ for the Cu–Cu segment and Cu atom and $k = 2$ for the Cu–Au segment and Au atom. The density matrix ρ for the cluster can be written in the form

$$\rho_{\text{clust}} = \exp\{-H_{\text{clust}}/kT\}/Z_{\text{clust}} \tag{10}$$

where Z_{clust} is a partial statistical sum for a cluster. Finally, the CVM equations can be written from the consistency conditions for the corresponding density matrices

$$Tr_{ij}\rho_{\text{tetrahedron}} = \rho_{\text{segment}} \tag{11}$$

$$Tr_i\rho_{\text{segment}} = \rho_{\text{site}}. \tag{12}$$

For the single sites the elements of the density matrix can be expressed through the mole fraction of Au atoms and long-range order parameter η (grand canonical ensemble)

$$\exp\left\{\frac{8\gamma_1 + h}{kT}\right\} - \exp\left\{\frac{-8\gamma_1 - h}{kT}\right\} = Z_1(2c - \tfrac{1}{2}\eta - 1) \tag{13}$$

and

$$\exp\left\{\frac{8\gamma_2 + h}{kT}\right\} - \exp\left\{\frac{-8\gamma_2 - h}{kT}\right\} = Z_2(2c + \tfrac{3}{2}\eta - 1). \tag{14}$$

The single particle statistical sums Z_1 and Z_2 are simply equal to the sum of the exponents in the left sides of equations (13) and (14). Solving the system of nonlinear equations (6)–(14) and returning back to the canonical ensemble one can calculate the Gibbs energy G and its derivatives. The corresponding concentration dependencies of the thermodynamic factor Φ for two temperatures below T_c are shown in Fig. 7. It can be seen that in the middle of the ordered region Φ is higher than in the disordered region. The amplitude of the Φ increase is higher at lower temperatures. Thus, in the CVM approximation the thermodynamic factor for interdiffusion is higher in the ordered alloy than in the disordered one.

4.2. *Comparison with experiment*

The A1–$L1_2$ phase transition in the Cu–Au system is of the first order and the corresponding two-phase areas exist in the phase diagram. Formally, the interdiffusion coefficient should go to zero there. However, we have not observed the rapid decrease of

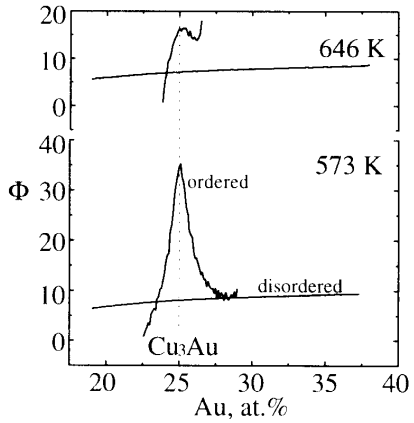

Fig. 7. The thermodynamic factor Φ as a function of the Au concentration for temperatures below the critical temperature of the order–disorder transformation T_{ord}, calculated in the tetrahedron approximation of CVM. The wavy character of the lines is caused by error accumulation during the calculations. The asymmetry of the maxima around 25 at.%Au are in accordance with the asymmetry in the composition range of the Cu_3Au phase [15]. The asymmetry is stronger for 646 K than for the 573 K.

$\tilde{D}$ at the boundaries of the ordered region. Indeed, in many cases narrow two-phase regions in the equilibrium phase diagram do not manifest themselves in the diffusion zone [15]. The minima on the $\tilde{D}(c)$ dependencies in the concentration interval 20–30 at.%Au above the critical point can be attributed by the short-range order influence on the diffusion process. The minimum on $\tilde{D}(c)$ at 25 at.%Au has been observed also at 773 K [25].

Other features of the $\tilde{D}(c)$ dependencies in Fig. 3 can be satisfactory described by the calculated $\Phi(c)$ dependencies:

- the $\tilde{D}(c)$ dependencies demonstrate a maxima in the interval of concentration 20–30 at.%Au below the critical point;
- the maxima are higher at lower temperatures;
- the maxima are shifted from the stoichiometric concentration of 25 at.%Au to higher Au concentrations. Though the maxima on the calculated $\Phi(c)$ dependencies are at approx. 25 at.%Au (see Fig. 7), the $\Phi(c)$ dependencies are strongly asymmetric, their gravity centre being shifted to higher Au concentrations, especially for higher temperatures.

It should be noted that the maxima in the concentration dependencies of the interdiffusion coefficient in Co_2Nb and Ni_3Nb intermetallics have been observed [9], and their presence has also been attributed to the thermodynamic factor. This is quite normal, because the intermetallic can be treated as a completely ordered binary alloy. It is interesting to mention that in Co_2Nb the maxima are shifted a little from the stoichiometric composition. In our study, the corresponding maxima are shifted by 2–3 at.% to the higher Au concentration, too.

In the above consideration we have ignored the possible role of the change of the tracer self-diffusion coefficients D^*_{Cu} and D^*_{Au} at the ordering. It follows from the atomistic theory of diffusion that in ordered Cu_3Au D^*_{Au} should drop rapidly in the ordered state because in the $L1_2$ ordered structure nearest neighbours of Au atoms are only Cu atoms, and the diffusional jump for the Au atom is connected with the creation of an antistructural defect [26]. It was recently shown [27] that the vacancy wind factor can be important in an ordered alloy. It exhibits a sharp minimum at the equiatomic composition. As we have not seen any noticeable decrease in the interdiffusion coefficient in the ordered region, any diffusion mechanism other than monovacancy jumps could be involved. For example, the unusually low values of the pre-exponential factor (see Fig. 5) indicate a strong correlation of the diffusion jumps [28]. Contrary to the vacancy wind factor and the tracer self-diffusion coefficient, the thermodynamic factor does not depend on the particular diffusion mechanism and describes only the trend of the alloy for mixing or unmixing. It should also be said that the magnetic effect for tracer diffusion has been observed in metals with body-centred cubic (b.c.c.) structure, which is more open than f.c.c. or hexagonal close-packed structures. There is no evidence for the magnetic effect in the f.c.c. Co or Ni [29]. Considering the analogy between magnetic and atomic ordering one can suppose only little change of tracer self-diffusion coefficients in the ordered state in the case of f.c.c. Cu–Au alloys. In any case, a corresponding negative contribution to the interdiffusion coefficient is lower when compared with the positive contribution of Φ, as Fig. 3 clearly shows.

It is clear from what is said above that the activation energy of interdiffusion has no physical sense in the concentration interval between 20 and 30 at.%Au. Unphysically low values of the activation energy (60 kJ/mol, see Fig. 3) can be explained by the strong temperature dependence of Φ: its lowering at temperatures above the critical point and its increase far below the critical point. The values of the activation energy and pre-exponential factor in the disordered region at a low Au concentration (120 ± 10 kJ/mol and 3×10^{-8} m^2/s) are in good agreement with the earlier data [30] for Au–Cu interdiffusion in the disordered region in the temperature interval 700–1000 K (115 kJ/mol and 6×10^{-8} m^2/s). The activation energy for the interdiffusion in the temperature interval 1006–1130 K [16] is higher (190 kJ/mol for Cu–Au alloys containing 10 and 20 at.%Au). Other values for the activation energy (42 kJ/mol for Cu–4 at.%Au alloy and 45 kJ/mol for Cu–8 at.%Au alloy) we have extracted from data in the literature [26] for the temperature interval 323–523 K. Thus, one can see that a strong scatter of the data for the activation energy of interdiffusion exists in the literature. It reflects the complex character of equation (4) for the

interdiffusion coefficient, which incorporates at least three temperature-dependent terms. By this, the activation energy can be dependent on the width of the temperature interval where the interdiffusion has been studied. The anomalies of Φ can, for example, explain the lowering of the activation energy for interdiffusion in Cu–50 at.%Au in the ordered state [31]. It was found that the activation energy in the ordered state (45 kJ/mol) is 20% lower than in the disordered state (57 kJ/mol).

5. SUMMARY AND CONCLUSIONS

The results of this study are summarized below, and the following conclusions can be drawn.

1. The interdiffusion coefficient $\tilde{D}$ has been determined for Cu–Au single crystalline alloys in the concentration range 5–40 at.%Au and temperature interval 573–673 K.
2. The concentration dependencies of the interdiffusion coefficient show in the concentration range 18–32 at.%Au the following features:
   - above the critical temperature $T_{ord} = 663$ K there are minima on these dependencies;
   - in the temperature interval 646–662 K the dependencies are monotonous;
   - below 646 K a maximum appears on these dependencies.
3. The thermodynamic factor Φ has been calculated in the tetrahedron approximation of the cluster variation method. Its concentration dependencies exhibit a maximum in the middle of the concentration interval of the ordered phase stability.
4. It is shown that the activation energy for interdiffusion has no physical sense in the interval of concentrations where the order–disorder phase transition occurs. The temperature dependence of the thermodynamic factor contributes strongly to the temperature dependence of the interdiffusion coefficient. Therefore, all data about activation energies and pre-exponential factors for interdiffusion measured near the phase transitions should be treated with care. The Arrhenius parameters for the interdiffusion in the disordered region (5–15 at.%Au) have been determined ($\tilde{Q} = 120 \pm 10$ kJ/mol and $\tilde{D}_0 = 3 \times 10^{-8}$ m^2/s).

Acknowledgements—The authors are very grateful to Dr T. Muschik for his help in producing the samples and the discussion of results, B.S. and E.R. wish to thank the Alexander-von-Humboldt Foundation for the financial support during this study. Professors L. S. Shvindlerman, H. Mehrer and Chr. Herzig are greatly acknowledged for productive discussions. We wish also to thank Dr E. Bischoff and Mrs B. Heiland for their help in processing the EPMA data.

REFERENCES

1. L. A. Johnson *et al.* (editors), *High-Temperature Ordered Intermetallic Alloys IV*, MRS Symp. Proc., Vol. 213. Mat. Res. Soc., Pittsburgh, (1991).
2. C. T. Liu *et al.* (editors), *Ordered Intermetallics—Physical Metallurgy and Mechanical Behavior*, NATO ASI Series E: Applied Sciences, Vol. 213. Kluwer Academic, Boston, Mass. (1992).
3. M. Yamaguchi and Y. Umakoshi, *Prog. Mater. Sci.* **34,** 1 (1990).
4. D. B. Miracle, *Acta metall. mater.* **41,** 649 (1993).
5. M. H. Yoo, S. L. Sass, C. L. Fu, M. J. Mills, D. M. Dimiduk and E. P. George, *Acta metall. mater.* **41,** 987 (1993).
6. F. C. Mix and F. E. Jaumont, *Phys. Res.* **83,** 1275 (1951).
7. H. Mehrer (editor), *Diffusion in Solid Metals and Alloys*, pp. 213 and 251. Landolt-Börnstein New Series Vol. III/26, Springer, Berlin (1992).
8. S. Shankar and L. L. Seigle, *Metall. Trans.* **9A,** 1467 (1978).
9. W. Sprengel, M. Denkinger and H. Mehrer, *Intermetallics* **2,** 137 (1994).
10. I. Richter and M. Feller-Kniepmeier, *Physica status solidi* (a) **68,** 289 (1981).
11. O. I. Noskovich, E. I. Rabkin, V. N. Semenov, B. B. Straumal and L. S. Shvindlerman, *Acta metall. mater.* **39,** 3091 (1991).
12. E. I. Rabkin, L. S. Shvindlerman and B. B. Straumal, *J. less-common Metals* **158,** 23, **159,** 43 (1990).
13. C. Nishimiura and C. T. Liu, *Acta metall. mater.* **40,** 723 (1992).
14. T. B. Massalski *et al.* (editors), *Binary Alloy Phase Diagrams*, p. 360. ASM International, Materials Park, Ohio (1990).
15. J. Philibert, *Atoms Movements—Diffusion and Mass Transport in Solids*, pp. 9, 211 and 424. Les Editions de Physique, Les Ulis (1991).
16. M. Badia and A. Vignes, *Met. Sci. Rev. Metall.* **66,** 915 (1969).
17. F. Sauer and V. Freise, *Z. Elektrochem.* **66,** 353 (1962).
18. L. Hall, *J. Chem. Phys.* **21,** 87 (1953).
19. J. R. Manning, *Phys. Rev. B* **4,** 1111 (1971).
20. G. Hettich, H. Mehrer and K. Maier, *Scripta Metall.* **11,** 795 (1977).
21. H. V. Mirani, R. Harthoorn, T. J. Zoorendonk, S. J. Helmenhorst and G. de Vries, *Physica status solidi* (a) **29,** 115 (1975).
22. J. Kucera, B. Kozak and H. Mehrer, *Physica status solidi* (a) **81,** 497 (1984).
23. A. B. Kuper, D. Lazarus, J. R. Manning and C. T. Tomizuka, *Phys. Rev.* **104,** 1936 (1956).
24. F. Ducastelle, *Order and Phase Stability in Alloys*, p. 187. Elsevier, Amsterdam (1991).
25. V. M. Polyanski, B. N. Podgorski and O. D. Makarovets, *Svar. Proizvod.* **3,** 9 (1971).
26. W. M. Young and E. W. Elcock, *Proc. Phys. Soc.* **89,** 735 (1966).
27. C. C. Wang and S. A. Akbar, in *Diffusion in Ordered Alloys* (edited by V. Fultz *et al.*), p. 3. Met. Min. Mat. Soc., Warrendale, Pa (1993).
28. B. S. Bokstein, *Diffusion in Metals*, p. 116. Metallurgia, Moscow (1978).
29. W. Petry, A. Heiming, J. Trampenau, M. Alla, Chr. Herzig, H. R. Schober and G. Vogl, *Phys. Rev. B* **43,** 10933 (1991).
30. W. Jost, *Z. Phys. Chem. B* **21,** 158 (1933).
31. M. Khobaib and K. P. Gupta, *Scripta metall.* **4,** 605 (1970).